[CANCER RESEARCH 64, 4481–4486, July 1, 2004]

Modulation of Tumor-host Interactions, Angiogenesis, and Tumor Growth by Tissue Inhibitor of Metalloproteinase 2 via a Novel Mechanism

Andrew L. Feldman,[1,2] William G. Stetler-Stevenson,[2,3] Nick G. Costouros,[1] Vladimir Knezevic,[4] Galina Baibakov,[4] H. Richard Alexander, Jr.,[1,3] Dominique Lorang,[1] Stephen M. Hewitt,[2] Dong-Wan Seo,[2] Marshall S. Miller,[1] Sarah O'Connor,[1] and Steven K. Libutti[1,3]

[1]Metabolism Section, Surgery Branch, [2]Laboratory of Pathology, and [3]Vascular Biology Faculty, Center for Cancer Research, National Cancer Institute, Bethesda, Maryland, and [4]20/20 Gene Systems, Inc., Rockville, Maryland

ABSTRACT

Solid tumors depend on angiogenesis for sustained growth. Tissue inhibitor of metalloproteinase 2 (TIMP-2) is an angiogenesis inhibitor initially characterized for its ability to block matrix metalloproteinases; however, recent data suggest that the antiangiogenic action of TIMP-2 may rely on matrix metalloproteinase-independent mechanisms. The aim of this study was to identify molecular pathways involved in the effects of TIMP-2 on processes dependent on tumor-host interactions such as angiogenesis. Using *in vitro* cell culture and a syngeneic murine tumor model, we compared the effects of TIMP-2 overexpression on gene expression profiles *in vitro* to those observed *in vivo*. Validating these findings by real-time quantitative PCR and layered protein scanning, we identified up-regulation of mitogen-activated protein kinase phosphatase 1 as an effector of the antiangiogenic function of TIMP-2. Up-regulation of mitogen-activated protein kinase phosphatase 1 in tumors overexpressing TIMP-2 leads to dephosphorylation of p38 mitogen-activated protein kinase and inhibition of tumor growth and angiogenesis. Phosphatase activity appears important in regulating tumor angiogenesis, offering a promising direction for the identification of novel molecular targets and antiangiogenic compounds for the treatment of cancer.

INTRODUCTION

Tissue inhibitor of metalloproteinase 2 (TIMP-2) is a multifunctional inhibitor of angiogenesis, tumor growth, and tumor invasion (1, 2). These processes involve not only tumor cells themselves but also the modulation of complex tumor-host interactions. Because the host response to the tumor microenvironment can act either to facilitate or to inhibit tumor invasion and spread, manipulating these host response elements has become a major focus of novel anticancer strategies (3, 4). Although TIMP-2 was initially characterized for its ability to block the action of matrix metalloproteinases (MMPs; Ref. 2), early clinical trials of synthetic small-molecule inhibitors of MMPs have been disappointing (5). Thus, the antiangiogenic action of TIMP-2 may rely on MMP-independent mechanisms that modulate tumor-host interactions (1, 6).

Angiogenesis is a prototypical example of the importance of tumor-host interactions because solid tumors are dependent on angiogenesis for continued growth (7). Prior studies have suggested that viable, potentially lethal tumor cells can remain dormant in the host for long periods of time if deprived of a neovasculature (8). Elucidation of molecular pathways involved in this and other tumor-host interactions may yield novel biological therapeutics for patients with cancer.

Received 9/16/03; revised 4/2/04; accepted 4/20/04.

The costs of publication of this article were defrayed in part by the payment of page charges. This article must therefore be hereby marked *advertisement* in accordance with 18 U.S.C. Section 1734 solely to indicate this fact.

Requests for reprints: Steven K. Libutti, Surgery Branch, National Cancer Institute, Building 10, Room 2B07, 10 Center Drive, Bethesda, MD 20892. Phone: (301) 496-5049; Fax: (301) 402-1788; E-mail: libuttis@mail.nih.gov.

MATERIALS AND METHODS

Overexpression of TIMP-2 in Murine Colon Adenocarcinoma Cells. pEF-null is a retroviral vector in which the downstream cytomegalovirus promoter of the vector pCLNCX has been replaced with the human elongation factor (EF)-1α promoter (9). The human TIMP-2 gene was cloned from the vector pBS-T2 (obtained from Dr. W. Stetler-Stevenson, National Cancer Institute) into the pEF-null vector to generate the vector pEF-T2. Pseudotyped retroviral particles were generated using pEF-null or pEF-T2 as described previously (9). MC38 murine colon adenocarcinoma cells (Surgery Branch, National Cancer Institute) were transduced with pEF-null- or pEF-T2-derived retroviral supernatant and cloned as described previously (9). Quantitative real-time PCR (qRT-PCR) was performed on RNA extracted from cells grown *in vitro* (see below for details). Transduced cell supernatants were tested using a human TIMP-2 ELISA (Amersham). A high TIMP-2-expressing clone, designated MC38/TIMP-2, was selected for further study. pEF-null-transduced cells were designated MC38/null. *In vitro* cell proliferation assays were performed as described previously (9).

***In Vivo* Tumor Growth and Microvascular Density.** Animal experiments were conducted according to protocols approved by the NIH Animal Care and Use Committee. Eight-week-old female C57BL/6 mice (Charles River Laboratories) received injections of 1×10^6 MC38, MC38/null, or MC38/TIMP-2 cells. Injections and tumor measurements were performed as described previously (9). To assess the effects of phosphatase inhibition, mice with tumors grown as above were treated with sodium orthovanadate (0.16 mg in 200 μl of PBS; Sigma) or PBS alone (200 μl) i.p., 5 days/week for 2 weeks, starting on day 14. Tumor sections were stained and microvascular density assessed as described previously (9).

RNA Isolation, qRT-PCR, and cDNA Microarray Analysis. For RNA isolation, cells cultured *in vitro* were resuspended in Trizol (Life Technologies, Inc.); harvested tumors were cleaned of peritumoral tissue and necrotic debris and homogenized in Trizol using a bead homogenizer (BIO 101). After the addition of chloroform, RNA was precipitated from the aqueous phase using isopropanol, washed in 70% ethanol, and resuspended in diethyl pyrocarbonate-H_2O. Concentration and purity of all RNA samples was determined using the $A_{260\ nm}/A_{280\ nm}$ ratio and formaldehyde gel electrophoresis. qRT-PCR was performed as described previously (10). Sequences were as follows: human *TIMP-2* (UniGene NM_003255)—5′-GAGCCTGAACCACAGGTACCA-3′, 5′-TCTGTGACCCAGTCCATCCA-3′, and 5′-FAM-AGTGCAAGATCACGCGCTGCCC-TAMRA-3′; and murine *Ptpn16* (NM_013642)—5′-GCGCGCTCCACTCAAGTC-3′, 5′-GCACAGCTCAGGGCAGGA-3′, and 5′-FAM-CCGAAAACGCTTCATATCCTCCTTGGA-TAMRA-3′.

The relative expression of each gene of interest was normalized to that of glyceraldehyde-3-phosphate dehydrogenase, and gene expression in each sample then was compared with expression in parental MC38 cells grown *in vitro*. Microarray analysis was conducted comparing gene expression in MC38/TIMP-2 and MC38/null cells *in vitro* and in MC38/TIMP-2 and MC38/null tumors after 6 or 12 days of s.c. growth. *In vivo* expression of the TIMP-2 gene at these time points was confirmed using qRT-PCR. cDNA microarray probes were synthesized using 30–50 μg of total RNA as described previously (10). All arrays were repeated using reciprocal fluorescence. Genes with an expression that differed between MC38/null and MC38/TIMP-2 by at least 2-fold in at least two of the four *in vivo* arrays were identified, and patterns of *in vitro* and *in vivo* gene expression were analyzed. Microarray findings for representative genes were validated by qRT-PCR.

Analysis of Tumor Protein Expression and Phosphorylation Status. For layered protein scanning (11), frozen sections (10-μm thickness) of tumor tissue were arrayed on a large glass slide and transferred onto 10 replicate membranes (20/20 Gene Systems) according to the manufacturer's recommendations. After transfer, membranes were gently washed in phosphate buffer (Pierce Biotechnology), incubated in 2 mg/ml EZ-Link Sulfo-NHS-Biotin (Pierce) in PBS for 30 min at room temperature, and washed in TBST buffer [50 mM TRIS (pH 8.0), 150 mM NaCl, and 0.05% Tween 20]. Membranes then were incubated in 1:500 dilution of streptavidin conjugated to fluorescein (Molecular Probes) for 15 min at room temperature, washed in TBST, and blocked for 15 min in 1× casein solution (Vector Laboratories). Membranes were incubated overnight at 4°C in one of the following primary antibodies: anti-p38 (1:100, Cell Signaling Technology); anti-phospho-p38 (1:100, Cell Signaling); or anti-mitogen-activated protein kinase phosphatase 1 (MKP-1; 1:100, Santa Cruz Biotechnology). The membranes then were washed in TBST, incubated in a complex of secondary antibody and alkaline phosphatase, and washed again. Localization of the target protein was visualized by enhanced chemiluminescence (DuoLux; Vector Laboratories) and Biomax MR film (Kodak). The images were digitalized by scanning on an Astra 2200 scanner (UMAX Technologies) and saved as TIFF files. After individual protein visualization, membranes were exposed to an Image Station CF440 (Kodak) to visualize biotinylated total protein and saved as TIFF files. Images were analyzed using MARKO Image Analysis Software (20/20 Gene Systems).

Immunoprecipitation and Western Blotting. Human microvascular endothelial cells were plated on gelatin-coated 100-mm dishes (BD Biosciences, San Jose, CA) in serum and growth factors (EGM-2 MV BulletKit; Cambrex, East Rutherford, NJ) for 24 h at 37°C, followed by an additional incubation for 24 h in serum-free EBM-2. Quiescent human microvascular endothelial cells were pretreated with 50 nM TIMP-2 for 20 min and stimulated with fibroblast growth factor 2 (50 ng/ml) for 15 min. After treatment, endothelial cells were rinsed twice with ice-cold PBS and lysed by incubation in 50 mM Tris-HCl (pH 7.4), 150 mM NaCl, 10% glycerol, 1% NP40, 1 mM EDTA, 100 μg/ml 4-(2-aminoethyl)benzenesulfonyl fluoride, 10 μg/ml aprotinin, 1 μg/ml pepstatin A, 0.5 μg/ml leupeptin, 80 mM β-glycerophosphate, 25 mM NaF, and 1 mM sodium orthovanadate for 30 min at 4°C. Cell lysates were clarified at 13,000 × g for 20 min at 4°C. For immunoprecipitation, 500 μg of whole cell lysates were incubated overnight with anti-mitogen-activated protein kinase (MAPK) antibody (Santa Cruz Biotechnology) followed by protein A/G PLUS-agarose (Santa Cruz Biotechnology), and the immunoprecipitates were resolved by SDS-PAGE and immunoblot analysis with anti-MKP-1 antibody (Santa Cruz Biotechnology).

Statistical Analysis. Groups were compared using the Mann-Whitney U test, and P values < 0.05 were considered statistically significant.

RESULTS AND DISCUSSION

Retroviral Transduction Yields Overexpression of TIMP-2 in MC38 Murine Colon Cancer Cells. To identify pathways involved in the host response to TIMP-2, we used retroviral gene transfer in a syngeneic murine tumor model. We previously incorporated the human EF-1α promoter into a modified retroviral vector and demonstrated prolonged antiangiogenic transgene expression in mice (9).

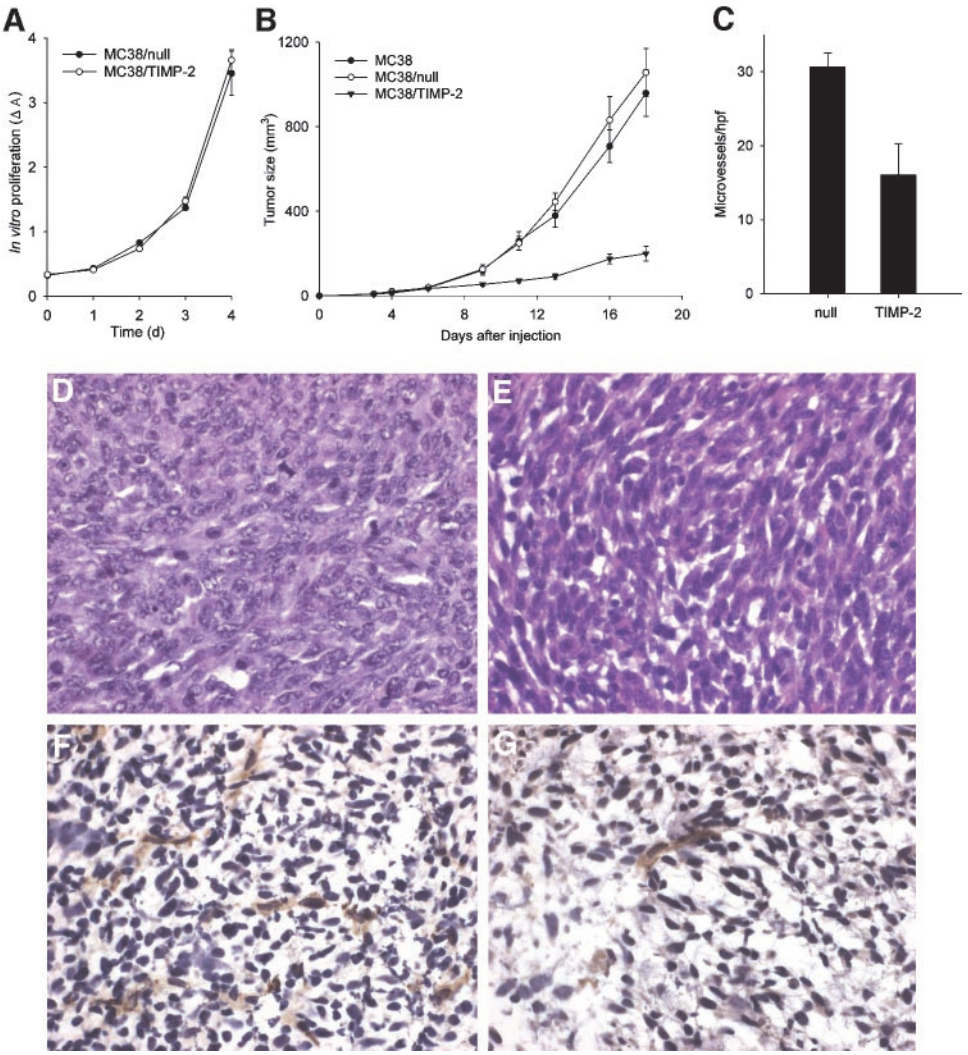

Fig. 1. Growth of murine colon cancer cells with and without overexpression of tissue inhibitor of metalloproteinase 2 (TIMP-2). *A*, murine adenocarcinoma cells were retrovirally transduced with a human TIMP-2 transgene (MC38/TIMP-2) or with an empty vector (MC38/null). An *in vitro* proliferation assay showed no significant differences in growth between the two cell lines [expressed as change in absorbance (ΔA)]. *B*, MC38/TIMP-2 tumors showed marked and sustained growth inhibition in mice compared with MC38/null tumors (tumor size at day 9: 54.8 ± 8.0 and 126.2 ± 20.9 mm^3, respectively, $P = 0.01$; day 18: 200.0 ± 34.8 and 1056.1 ± 112.9 mm^3, respectively, $P = 0.0008$; $n = 8$ mice/group). *C*, angiogenesis was significantly reduced in MC38/TIMP-2 tumors compared with MC38/null tumors (16.1 ± 4.2 and 30.7 ± 1.9 CD31-positive microvessels/×600 high power field (hpf), respectively; $P < 0.05$; $n = 5$ tumors/group). MC38/null (*D*) and MC38/TIMP-2 (*E*) showed similar tumor morphology (H&E, ×400). *F*, MC38/null tumors demonstrated scattered CD31-positive microvessels (brown reaction product, ×400), compared with a relative paucity of microvessels in MC38/TIMP-2 tumors (*G*).

Continuous release of an antiangiogenic protein, as can be achieved using a retroviral gene transfer model, appears more effective than intermittent bolus dosing (12). The human TIMP-2 gene was cloned into the empty vector pEF-null, and MC38 murine colon adenocarcinoma cells were transduced with pseudotyped retroviral particles. A high TIMP-2-expressing clone (MC38/TIMP-2) was selected for further study. MC38/TIMP-2 cells grown *in vitro* demonstrated a 14-fold increase in TIMP-2 RNA as determined by qRT-PCR. Mean TIMP-2 protein concentrations in the supernatants of MC38/TIMP-2 cells were 136 ng/ml as determined by ELISA.

TIMP-2 Overexpression Inhibits MC38 Tumor Growth *in Vivo* but not *in Vitro*. We then evaluated MC38/TIMP-2 growth *in vitro* and *in vivo*. In a 4-day *in vitro* proliferation assay, there were no significant differences in growth between MC38/TIMP-2 and MC38/null cells (Fig. 1*A*). However, three-dimensional tumor size after s.c. injection into syngeneic mice revealed substantial growth inhibition of the MC38/TIMP-2 tumors compared with either MC38/null or wild-type MC38 tumors (Fig. 1*B*). This difference was statistically significant 9 days after tumor cell inoculation and became progressively more dramatic until control animals required sacrifice. A lesser degree of growth inhibition was seen when mice were inoculated with bulk TIMP-2-transduced MC38 cells or a transduced MC38 clone with lower TIMP-2 expression (data not shown). This finding suggests a dose effect of TIMP-2-induced growth inhibition. The high-expressing MC38/TIMP-2 clone demonstrated similar growth inhibition in nude mice as in immunocompetent mice (data not shown), suggesting that tumor inhibition was not caused by immunogenicity. Because MC38/TIMP-2 growth was inhibited only *in vivo* and not *in vitro*, we concluded that tumor-host interactions are responsible for TIMP-2-induced tumor growth inhibition.

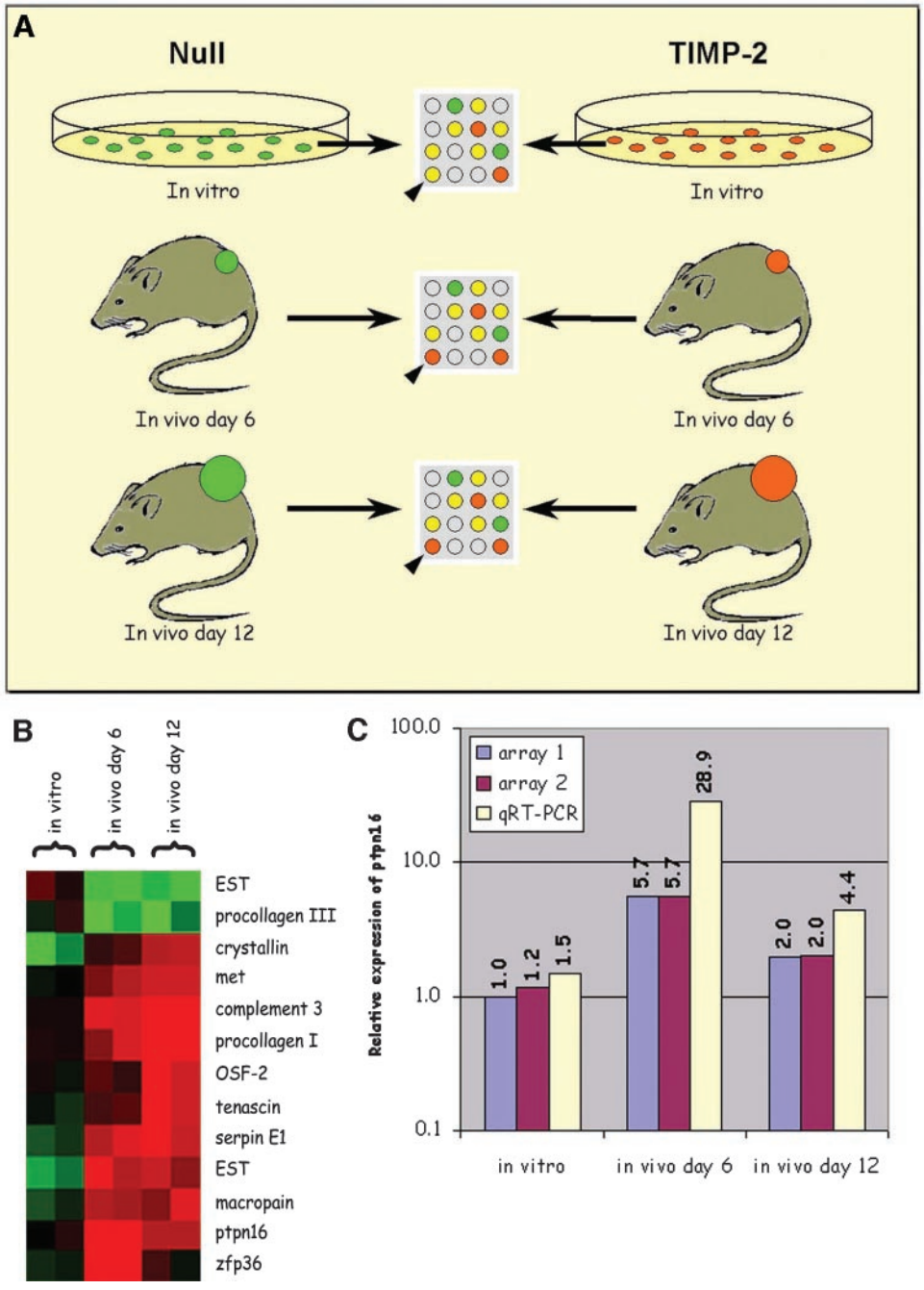

Fig. 2. Identification of genes associated with the host response to tissue inhibitor of metalloproteinase 2 (TIMP-2). *A*, strategy for comparing gene expression patterns of MC38/null and MC38/TIMP-2 tumor cells *in vitro* and *in vivo*. Using cDNA microarrays, MC38/null (*green*) and MC38 TIMP-2 (*red*) were compared *in vitro* and *in vivo* after 6 or 12 days of growth. Genes associated with tumor-host interactions caused by TIMP-2 might be similarly expressed *in vitro* (*e.g.*, *yellow spot* in bottom left corner of top array, *arrowhead*) but differentially expressed *in vivo* (*red spot* in bottom left corner of bottom two arrays, *arrowheads*). *B*, cDNA microarray analysis identified 13 such genes. Each pixel represents the expression ratio on one array. *Red* indicates up-regulation in the MC38/TIMP-2 sample, and *green* indicates down-regulation. Color intensity is proportional to expression ratio. *Black* represents ratios close to 1.0. *C*, microarray and quantitative real-time PCR (qRT-PCR) data for Ptpn16, the murine gene for mitogen-activated protein kinase phosphatase 1. Relative expression of Ptpn16 refers to the ratio of gene expression in MC38/TIMP-2 tumors compared with that in MC38/null tumors. Ptpn16 expression ratios were close to 1.0 *in vitro* but showed up-regulation in MC38/TIMP-2 tumors *in vivo*.

TIMP-2 Overexpression Inhibits Tumor Angiogenesis *in Vivo*. Because TIMP-2 inhibits endothelial cells (13–15), we evaluated the effects of TIMP-2 overexpression on *in vivo* tumor angiogenesis. Microvessel counts based on CD31-immunostained tumor sections revealed a statistically significant reduction in microvascular density in MC38/TIMP-2 tumors compared with MC38/null tumors ($P < 0.05$; Fig. 1*C*). The difference in microvascular density was observed on immunostained sections despite similar tumor morphology (Fig. 1*D–G*). MC38/TIMP-2 also demonstrated less vascularity grossly. Thus, TIMP-2 overexpression inhibits tumor angiogenesis.

Comparison of Gene Expression Profiles *in Vitro* and *in Vivo* Yields Candidate Host Response-Associated Genes. Because of the striking phenotypic difference in growth between TIMP-2-transduced tumor cells grown *in vivo* and those grown *in vitro*, we sought to identify genes associated with tumor-host interactions induced by TIMP-2. Results from cDNA microarrays performed on *in vitro* cell lines were compared with those performed on *in vivo* tumors. Because the growth curves of MC38/TIMP-2 and MC38/null tumors diverged between days 6 and 12 after inoculation (Fig. 1*B*), these two time points were selected for *in vivo* gene expression analysis. Earlier time points might fail to identify critical pathways responsible for antitumor effects, whereas later time points might identify nonspecific secondary effects related to unchecked tumor growth in controls. TIMP-2 mRNA remained increased in MC38/TIMP-2 tumors during the time course studied (6.3–7.2-fold up-regulation by qRT-PCR).

A schematic diagram of the approach to cDNA microarray analysis is shown in Fig. 2*A*. MC38/TIMP-2 cells were compared with MC38/null cells *in vitro* and after 6 or 12 days of *in vivo* growth. For each comparison, duplicate arrays were performed, and genes were identified as differentially expressed *in vivo* if they were altered ≥2-fold in at least half of the arrays performed on *in vivo* samples. In addition, genes were considered differentially expressed only if expression ratios reciprocated when the red and green fluorophores were reversed. Using these criteria, 28 genes were found to be differentially expressed *in vivo* (*i.e.,* up- or down-regulated in MC38/TIMP-2 tumors compared with MC38/null tumors). Of these 28 genes, 8 showed similar expression differences *in vitro*, suggesting alterations in the tumor cells themselves, rather than in tumor-host interactions. Seven genes showed expression patterns that changed between days 6 and 12; these genes were not additionally analyzed. The remaining 13 genes showed persistent expression differences *in vivo* that were not present *in vitro* and were considered candidates for genes related to tumor-host interactions induced by TIMP-2 (Fig. 2*B*).

To select genes for further study, we reviewed the known relationships between each gene and TIMP-2-related processes such as angiogenesis and invasion. Of particular interest was Ptpn16, the murine gene for MKP-1, a dual specificity phosphatase involved in the dephosphorylation (and thus inactivation) of a number of tyrosine and threonine kinases involved in signal transduction in response to growth stimuli, including MAPKs (16). We and others (1, 6) have previously suggested the potential importance of phosphatases in TIMP-2-induced inhibition of angiogenesis. We hypothesized that up-regulation of Ptpn16 might be a critical event in TIMP-2-induced inhibition of tumor growth via inactivation of MAPK pathways. It is important to emphasize that in this regard the microarray data are being used only as a screening tool for generating testable hypotheses and not as an end point in themselves. Array data suggested that Ptpn16 was up-regulated >5-fold in MC38/TIMP-2 tumors, even when tumors had not yet shown gross evidence of growth inhibition (day 6; Fig. 2*C*). qRT-PCR suggested Ptpn16 up-regulation might be much higher (~30-fold), a phenomenon we reported previously (10). Ptpn16 expression ratios remained increased at day 12, although to a lesser degree than at day 6. With only two time points assayed, it is difficult to speculate on the reason for this drop, although it is likely that mediators other than TIMP-2 regulate the expression of Ptpn16. Perhaps as the control tumors grow, other antiangiogenic mediators cause up-regulation of Ptpn16, or perhaps feedback loops in the TIMP-2-transduced tumors temper Ptpn16 expression over time.

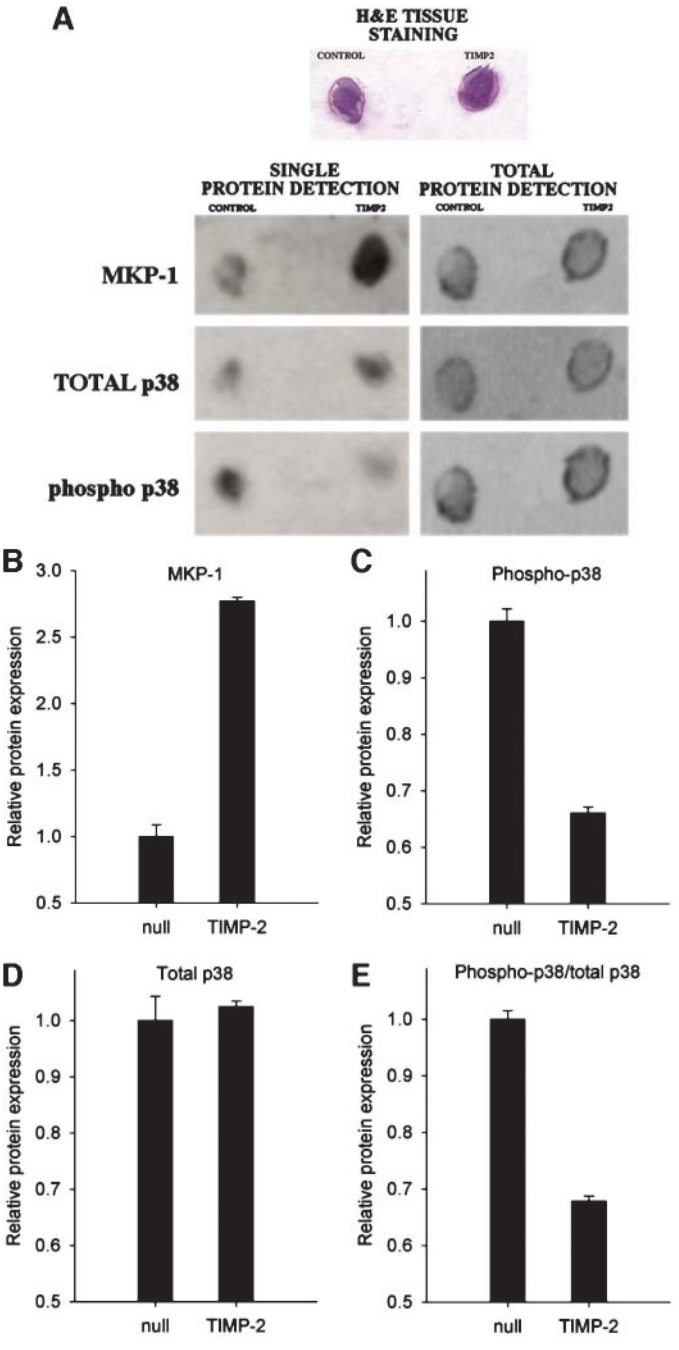

Fig. 3. Layered protein scanning of tissue arrays. *A,* multiple tumor sections were arrayed on a glass slide. A portion of the array is shown, demonstrating H&E-stained sections of MC38/TIMP-2 and control (MC38/null) tumors. Proteins were transferred to replicate layered membranes, which were probed using antibodies to mitogen-activated protein kinase phosphatase 1 (MKP-1), total p38, and phospho-p38 (single protein detection, *left*). Images were scanned, and values were normalized to total protein (*right*). *B,* expression of MKP-1, the Ptpn16 gene product, was increased by a factor of 2.8 in MC38/TIMP-2 tumors compared with MC38/null tumors. *C,* expression of the phosphorylated form of p38 mitogen-activated protein kinase, subject to dephosphorylation by MKP-1, was decreased by 34% in MC38/TIMP-2 tumors, whereas total p38 expression (*D*) was similar. *E,* thus, a 32% overall decrease in p38 phosphorylation, expressed as the phospho-p38/total p38 ratio, was seen in the MC38/TIMP-2 tumors.

TIMP-2-Induced MKP-1 Expression Is Associated with Inhibition of Tumor Growth and Decreased Phosphorylation of p38 MAP Kinase. To analyze protein expression patterns associated with the gene expression profile results described above, we used layered protein scanning (11), a multireplica protein-blotting technique, to produce replicate membranes of a tissue array representing multiple sections of three tumors from each experimental group (between five and nine total sections/group; Fig. 3*A*). These membranes were probed with specific antibodies, and the resultant signals were quantified, normalized to total protein, and expressed as relative protein with respect to control (MC38/null) tumors. MKP-1 protein expression was increased 2.8-fold in MC38/TIMP-2 tumors (Fig. 3*B*). Western blotting of protein lysates from null- and TIMP-2-transduced tumor cells grown *in vitro* yielded bands of similar intensity when probed for MKP-1 (data not shown). These findings suggest a link between MKP-1 up-regulation and TIMP-2-associated inhibition of angiogenesis *in vivo*, although the cell of origin of the increased MKP-1 expression *in vivo* cannot be ascertained definitively from these data. Because MKP-1 dephosphorylates MAPK pathways (16, 17), membranes were probed for total and phosphorylated p38 MAPK. p38 MAPK plays a critical role in signal transduction in response to various angiogenic molecules, including fibroblast growth factor and vascular endothelial growth factor (18–20), and p38 MAPK inhibitors have been shown to be directly antiangiogenic (21). Layered protein scanning demonstrated a 34% decrease in phosphorylated p38 in MC38/TIMP-2 tumors (Fig. 3*C*), whereas total p38 was unchanged (Fig. 3*D*). This corresponded to an overall decrease in the phospho-p38/total p38 ratio of 32% in MC38/TIMP-2 tumors ($P = 0.0005$; Fig. 3*E*).

To verify that the TIMP-2-associated decrease in p38 phosphorylation was associated with increased phosphatase activity and tumor growth inhibition, we treated MC38/TIMP-2 tumor-bearing mice with orthovanadate, an inhibitor of phosphatases, including MKP-1 (22, 23). Growth of TIMP-2-transduced tumors was accelerated during orthovanadate treatment (Fig. 4*A*), whereas the tumor growth curves converged after cessation of orthovanadate administration. Growth

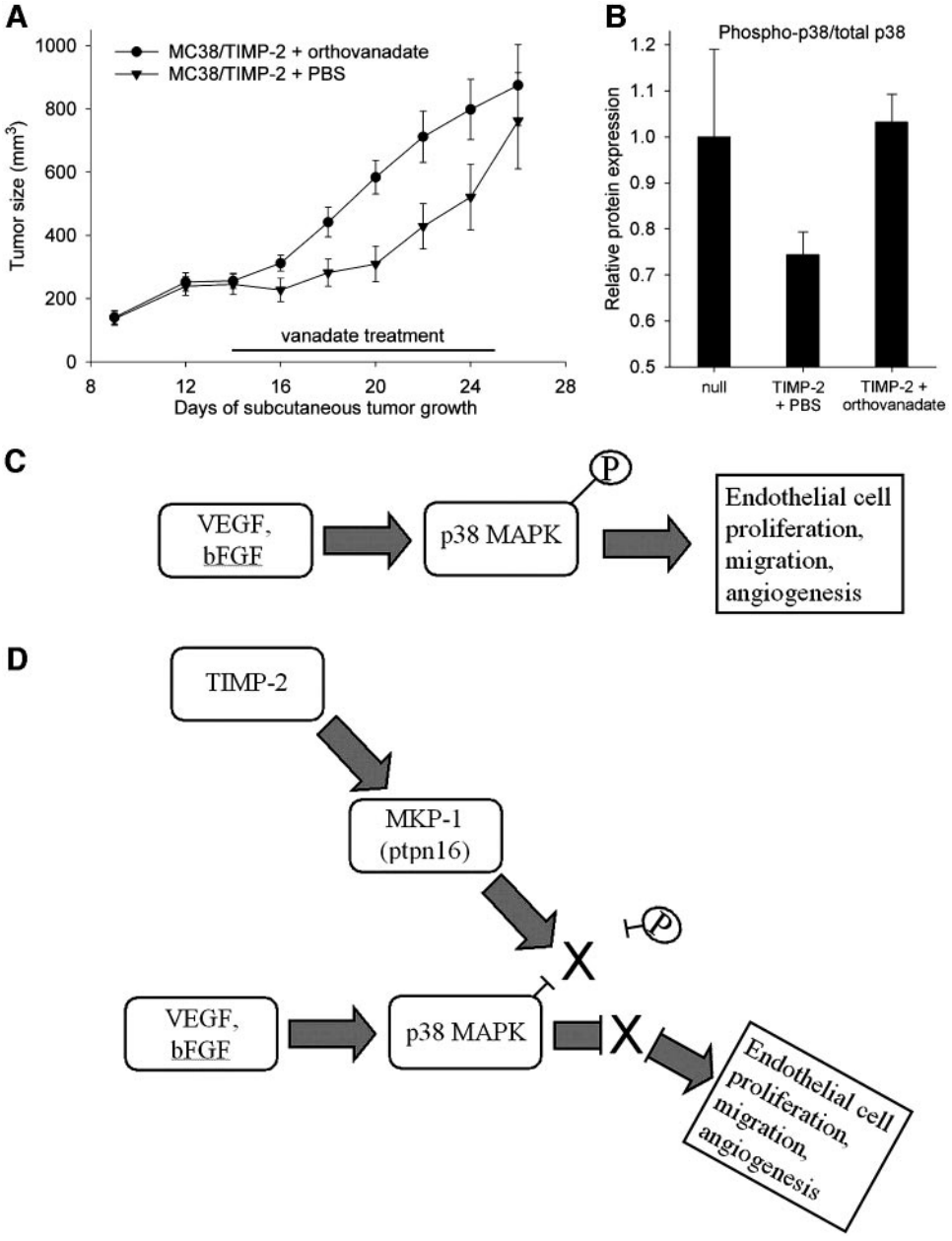

Fig. 4. Role of mitogen-activated protein kinase phosphatase 1 (MKP-1) in tissue inhibitor of metalloproteinase 2 (TIMP-2) mechanism of action. *A*, treatment with the phosphatase inhibitor orthovanadate accelerated growth of MC38/TIMP-2 tumors (tumor volumes after 1 week of treatment, 584 ± 53 and 309 ± 56 mm^3, respectively; $P = 0.004$). *B*, orthovanadate injection completely reversed the TIMP-2-induced dephosphorylation of p38 mitogen-activated protein kinase (MAPK). Taken together, these data suggest a mechanism for the effects of TIMP-2 on angiogenesis and other host response elements. *C*, proangiogenic factors such as vascular endothelial growth factor (VEGF) and basic fibroblast growth factor (bFGF) are known to stimulate endothelial cell proliferation and migration in part by activating MAPK pathways, including p38. *D*, TIMP-2 may inactivate p38 MAPK through the up-regulation of MKP-1, dephosphorylating p38, and preventing signal transduction of proangiogenic stimuli from cytokines in the tumor microenvironment.

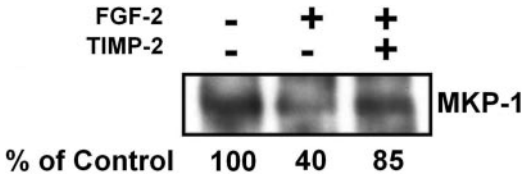

Fig. 5. Effects of tissue inhibitor of metalloproteinase 2 (TIMP-2) on mitogen-activated protein kinase phosphatase 1 (MKP-1) binding to mitogen-activated protein kinase phosphatase (MAPK). Immunoprecipitation was performed on endothelial cell protein lysates using a polyclonal antibody to MAPK, and coprecipitated MKP-1 was analyzed by Western blotting. Band densities from immunoprecipitated fibroblast growth factor (FGF)-stimulated endothelial cell lysates were quantified and compared with those from unstimulated cell lysates (control, *left lane*). FGF-stimulated endothelial cells grown in the presence of TIMP-2 (*right lane*) showed a >2-fold increase in MKP-1 bound to MAPK compared with cells grown without TIMP-2 (*center lane*).

curves of MC38/null tumors were similar to those shown in Fig. 1*B*, *i.e.*, MC38/null tumor grew more rapidly than MC38/TIMP-2 tumors with or without orthovanadate, indicating that orthovanadate only partially reversed the TIMP-2-induced tumor growth inhibition. At the molecular level, however, layered protein scanning of orthovanadate- and PBS-treated tumors demonstrated that orthovanadate completely reversed the TIMP-2-induced decrease in p38 MAPK phosphorylation in MC38/TIMP-2 tumors ($P = 0.003$ *versus* PBS-treated animals; Fig. 4*B*). These findings suggest a mechanism of TIMP-2 action whereby induction of MKP-1 leads to inactivation of MAPK pathways and inhibition of angiogenesis and tumor growth (Fig. 4, *C* and *D*). The antiangiogenic effects of TIMP-2 might additionally increase MKP-1 expression by inducing intratumoral hypoxia (24).

To determine whether the TIMP-2-induced increase in MKP-1 occurs in endothelial cells, we examined MKP-1 expression in protein lysates from fibroblast growth factor-stimulated endothelial cells grown *in vitro*. MKP-1 exerts its effects by binding to MAPKs and dephosphorylating them. Therefore, we performed immunoprecipitation using an anti-MAPK polyclonal antibody and examined the amount of MKP-1 that was coprecipitated. The addition of TIMP-2 to the endothelial cell medium caused a >2-fold increase in the amount of MKP-1 bound to MAPK in the cell lysate (Fig. 5). These data show that TIMP-2 has direct effects on MKP-1 in endothelial cells and support the hypothesis that MKP-1-induced MAPK inactivation contributes to the antiangiogenic effects of TIMP-2.

These findings are in agreement with our recent study that TIMP-2 directly inhibits microvascular endothelial cell growth and angiogenesis via a mechanism that is independent of MMP inhibition but requires integrin binding and protein tyrosine phosphatase activity (6). These data demonstrated that TIMP-2 suppresses phosphorylation of endothelial cell receptors for fibroblast growth factor (FGFR-1) and vascular endothelial growth factor (KDR) in a phosphatase-dependent manner. Combined with data from the present study, it appears that TIMP-2 may inactivate growth signaling pathways in endothelial cells by modulating the expression or activity of phosphatases that act at multiple key points along these pathways. Development of a therapeutic agent to duplicate this antiangiogenic mechanism of TIMP-2 may be critical to augment clinical efficacy of small-molecule MMP inhibitors.

In conclusion, we demonstrate that the antiangiogenic action of TIMP-2 is mediated in part by the induction of MKP-1, leading to p38 MAPK pathway inactivation. In addition, we present these findings as a general strategy to identify molecular pathways associated with the host response to the tumor microenvironment. In the era of molecular therapies specific to cancer-related biological processes, identifying novel molecular targets has become a central focus of experimental anticancer therapeutics. As with many signal transduction pathways governing cellular responses to growth stimuli, the p38 MAPK pathway is phosphorylation dependent, and changes in its activation status might be overlooked by strategies which address only gene expression or even total protein expression. However, gene expression profiling can identify regulatory genes such as Ptpn16, which may impact phosphorylation of signaling genes and thus can generate testable hypotheses that lead to identification of critical molecular targets through downstream proteomic analysis. We also emphasize that at the initial time point studied, tumors in all groups were of identical size. Thus, this approach can identify molecular differences in tumors exposed to inhibitory agents before gross differences in tumor growth are noted. Specifically, the identification of MKP-1 as a modulator of the *in vivo* antiangiogenic action of TIMP-2 suggests new molecular targets for the development of more effective antiangiogenic drugs, and such efforts are currently underway in our laboratory.

REFERENCES

1. Hoegy SE, Oh HR, Corcoran ML, Stetler-Stevenson WG. Tissue inhibitor of metalloproteinases-2 (TIMP-2) suppresses TKR-growth factor signaling independent of metalloproteinase inhibition. J Biol Chem 2001;276:3203–14.
2. Stetler-Stevenson WG. Matrix metalloproteinases in angiogenesis: a moving target for therapeutic intervention. J Clin Investig 1999;103:1237–41.
3. Feldman AL, Libutti SK. Antiangiogenesis. In: Lotze MT, editor. The cytokine handbook. London: Elsevier; 2003. p. 1279–95.
4. Liotta LA, Kohn EC. The microenvironment of the tumour-host interface. Nature (Lond.) 2001;411:375–9.
5. Zucker S, Cao J, Chen WT. Critical appraisal of the use of matrix metalloproteinase inhibitors in cancer treatment. Oncogene 2000;19:6642–50.
6. Seo DW, Li H, Guedez L, et al. TIMP-2 mediated inhibition of angiogenesis: an MMP-independent mechanism. Cell 2003;114:171–80.
7. Folkman J. What is the evidence that tumors are angiogenesis dependent? J Natl Cancer Inst (Bethesda) 1990;82:4–6.
8. Holmgren L, O'Reilly MS, Folkman J. Dormancy of micrometastases: balanced proliferation and apoptosis in the presence of angiogenesis suppression. Nat Med 1995;1:149–53.
9. Feldman AL, Alexander HR, Hewitt SM, et al. Effect of retroviral endostatin gene transfer on subcutaneous and intraperitoneal growth of murine tumors. J Natl Cancer Inst (Bethesda) 2001;93:1014–20.
10. Feldman AL, Costouros NG, Wang E, et al. Advantages of mRNA amplification for microarray analysis. Biotechniques 2002;33:906–12, 914.
11. Englert CR, Baibakov GV, Emmert-Buck MR. Layered expression scanning: rapid molecular profiling of tumor samples. Cancer Res 2000;60:1526–30.
12. Kisker O, Becker CM, Prox D, et al. Continuous administration of endostatin by intraperitoneally implanted osmotic pump improves the efficacy and potency of therapy in a mouse xenograft tumor model. Cancer Res 2001;61:7669–74.
13. Hajitou A, Sounni NE, Devy L, et al. Down-regulation of vascular endothelial growth factor by tissue inhibitor of metalloproteinase-2: effect on *in vivo* mammary tumor growth and angiogenesis. Cancer Res 2001;61:3450–7.
14. Schnaper HW, Grant DS, Stetler-Stevenson WG, et al. Type IV collagenase(s) and TIMPs modulate endothelial cell morphogenesis *in vitro*. J Cell Physiol 1993;156:235–46.
15. Murphy AN, Unsworth EJ, Stetler-Stevenson WG. Tissue inhibitor of metalloproteinases-2 inhibits bFGF-induced human microvascular endothelial cell proliferation. J Cell Physiol 1993;157:351–8.
16. Keyse SM. Protein phosphatases and the regulation of MAP kinase activity. Semin Cell Dev Biol 1998;9:143–52.
17. Kiemer AK, Weber NC, Furst R, Bildner N, Kulhanek-Heinze S, Vollmar AM. Inhibition of p38 MAPK activation via induction of MKP-1: atrial natriuretic peptide reduces TNF-alpha-induced actin polymerization and endothelial permeability. Circ Res 2002;90:874–81.
18. Lee OH, Bae SK, Bae MH, et al. Identification of angiogenic properties of insulin-like growth factor II in *in vitro* angiogenesis models. Br J Cancer 2000;82:385–91.
19. Rousseau S, Houle F, Landry J, Huot J. p38 MAP kinase activation by vascular endothelial growth factor mediates actin reorganization and cell migration in human endothelial cells. Oncogene 1997;15:2169–77.
20. Tanaka K, Abe M, Sato Y. Roles of extracellular signal-regulated kinase 1/2 and p38 mitogen-activated protein kinase in the signal transduction of basic fibroblast growth factor in endothelial cells during angiogenesis. Jpn J Cancer Res 1999;90:647–54.
21. Jackson JR, Bolognese B, Hillegass L, et al. Pharmacological effects of SB 220025, a selective inhibitor of P38 mitogen-activated protein kinase, in angiogenesis and chronic inflammatory disease models. J Pharmacol Exp Ther 1998;284:687–92.
22. Charles CH, Sun H, Lau LF, Tonks NK. The growth factor-inducible immediate-early gene 3CH134 encodes a protein-tyrosine-phosphatase. Proc Natl Acad Sci USA 1993;90:5292–6.
23. Lin WW, Hsu YW. Cycloheximide-induced cPLA(2) activation is via the MKP-1 down-regulation and ERK activation. Cell Signal 2000;12:457–61.
24. Seta KA, Kim R, Kim HW, Millhorn DE, Beitner-Johnson D. Hypoxia-induced regulation of MAPK phosphatase-1 as identified by subtractive suppression hybridization and cDNA microarray analysis. J Biol Chem 2001;276:44405–12.